**Supporting Information**

# Injectable self-healing hydrogels loaded with Crinis Carbonisatus nanoparticles for rapid hemostasis and wound healing

Rui Tian,[ab] Fazhen Luo,[b] Yilin Yu,[b] Jinxia Mi,[b] Xiaoya Gao,[b] Zhengtao Wang *[a] and Yan Xie *[b]

[a] Institute of Chinese Materia Medica, Shanghai University of Traditional Chinese Medicine, Shanghai 201203, China

[b] Research Center for Health and Nutrition, Shanghai University of Traditional Chinese Medicine, Shanghai 201203, China

## 1. Methods

*1.1. Synthesis of HPCS-C with different degrees of catechol group grafting*

The synthesis of HPCS-C with different degrees of catechol group grafting was achieved by controlling the ratio of HPCS to HAC. Briefly, 364, 728, and 1456 mg of HAC were dissolved in 10 mL of deionized water and added dropwise to 100 mL of a 1% (v/v) aqueous solution of HPCS, respectively. Then, EDC (1:1 molar ratio to HAC) and NHS (1:1 molar ratio to HAC) were dissolved in 100 mL of 50% (v/v) aqueous ethanol, added dropwise to the HPCS and HAC mixture, and the pH was adjusted to 5.0. The reaction mixture was sealed and stirred for 20 hours at room temperature. The resulting solution was dialyzed in a dialysis tube (MWCO: 3500 Da) against deionized water at pH 5 for 2 days and then dialyzed twice with deionized water. The final HPCS-C product was lyophilized and stored at -20°C. The grafting rates of the synthesized HPCS-C catechol molecules were 6.27%, 6.94%, and 9.95% as determined by UV spectroscopy and were named HPCS-C-L, HPCS-C-M, and HPCS-C-H, respectively.

*1.2. Determination of cross-linking degree*

The degree of cross-linking degree was determined based on the method of Wang et al. [1] with small modifications. Firstly, 8 mg of lyophilized HPCS-C/ODEX/CC hydrogels or 5 mg of HPCS-C were heated with 1 mL of 4% $NaHCO_3$ solution (pH=8.5) and 1 mL of 0.5% TNBS at 40°C for 2 h. Subsequently, after the addition of 3 mL of 6 M HCl, the mixtures were maintained at 60°C for 2 h to terminate the reaction. Finally, the reaction solution was diluted 10-fold with deionized water and the absorbance was measured at 344 nm. The degree of cross-linking of the hydrogel was calculated according to the following formula:

$$cross-linking\ degree(\%) = A_{NH2} - A_{NHCross}/A_{NH2} \times 100\%$$

where: $A_{NH2}$ is the absorbance of the uncross-linked sample and $A_{NHcross}$ is the absorbance of the cross-linked sample.

*1.3. Rheology and self-healing behaviors*

The hydrogels were injected onto the platform of the rheometer, 25 mm parallel plates were selected, and the gap distance was set to 1.0 mm for rheological testing at room temperature. A frequency sweep was conducted, measuring from 0.1 to 100 rad/s

with a fixed strain of 1%. Amplitude scans were conducted at a constant angular frequency (ω) of 0.1 Hz, with a strain range of 0.01-1000%. Subsequently, a shear rate scan was conducted to document the alteration in viscosity from 0.1 to 100 $s^{-1}$. Moreover, the self-healing capacity of the hydrogels was investigated through alternating step-strain scanning tests. Specifically, a fixed corner frequency of 1 Hz was employed to alternate the strain between 1% and 500% in a stepwise manner. Each strain was maintained for 120 seconds at each level for a total of three cycles.

Macroscopic self-healing behaviors were performed to evaluate the self-healing performance of hydrogels. Briefly, the HPCS-C/ODEX hydrogel was cut into two parts with a razor blade and stained with red and blue dyes, respectively. The fractured portions were then touched together without applying stress and left at room temperature for 30 minutes. The self-healing properties of the hydrogels were assessed by visual inspection.

*1.4. Adhesion test*

Fresh pig skin was cut into long strips of 50 mm × 10 mm. Different hydrogels were injected into the inner layer of the pig skin and the contact area with the skin was controlled to be 10 mm × 10 mm, followed by covering another piece of pig skin with the hydrogel. After pressing with a load of 100 g for 1 hour, lap shearing was performed using a universal testing machine (Instron 5943, Instron, USA).

*1.5. Antioxidant activity assessment*

In brief, 100 μM DPPH and the desired amount of CC nanoparticles or different hydrogel samples were dispersed in 4.0 mL of ethanol. The mixture was stirred and incubated in the dark for 30 minutes at room temperature. The absorption of the DPPH mixture was then measured using a UV – vis spectrophotometer (Agilent 8453, Agilent Technologies, USA). The scavenging of DPPH was calculated using the following formula:

$$Scavenging\ of\ DPPH\ (\%) = (A_B - A_S)/A_B \times 100\%$$

where $A_B$ and $A_S$ are the absorbance of the blank (DPPH + ethanol) and the samples (DPPH + ethanol + samples) at 517 nm, respectively.

For the ABTS free radical scavenging assay, 7 mM of ABTS and 2.6 mM of potassium persulfate were mixed in a 1:1 (v/v) ratio and reacted for 12 hours in the dark. The reaction solution was diluted with PBS until its absorbance value reached 0.7 at 734 nm, forming the ABTS working solution. Subsequently, 1 mg of the sample was added to 6 mL of the ABTS working solution and allowed to react for 6 minutes. The absorbance was then measured at 734 nm, and the scavenging of ABTS was calculated using the following equation:

$$Scavenging\ of\ ABTS\ (\%) = (A_B - A_S)/A_B \times 100\%$$

where $A_B$ and $A_S$ are the absorbance of the blank (ABTS working solution) and the samples (ABTS working solution+ samples) at 734 nm, respectively.

*1.6. Cytocompatibility*

The cytotoxicity of the hydrogels was assessed using an MTS assay by co-culturing hydrogel extracts with the mouse epithelioid fibroblast cell line L929 *in vitro*. In brief, the L929 cells were seeded at a density of $1 \times 10^5$ cells per well in a 96-well plate and cultured for 24 h in a 37°C incubator with a 5% $CO_2$ atmosphere. The cells were then treated with 100 μL of hydrogel extract and cultured for 1, 3, and 5 days. Subsequently, 120 μL MTS solution (MTS: DMEM = 1: 5) was added to each well and incubated for 1 hour. The absorbance at 490 nm was measured using a Multiskan Spectrum microplate reader (Thermo Fisher Scientific, USA).

Cell viability and morphology were assessed using a Live/Dead assay with acridine orange/ethidium bromide (AO/EB) double staining. After incubation for 1, 3, and 5 days, L929 cells were washed with PBS three times and then incubated with Live/Dead staining media for 10 minutes. They were then observed under an ImageXpress Micro 4 high-content imaging analysis system (Molecular Devices, USA). Live cells were stained green, while dead cells were stained red.

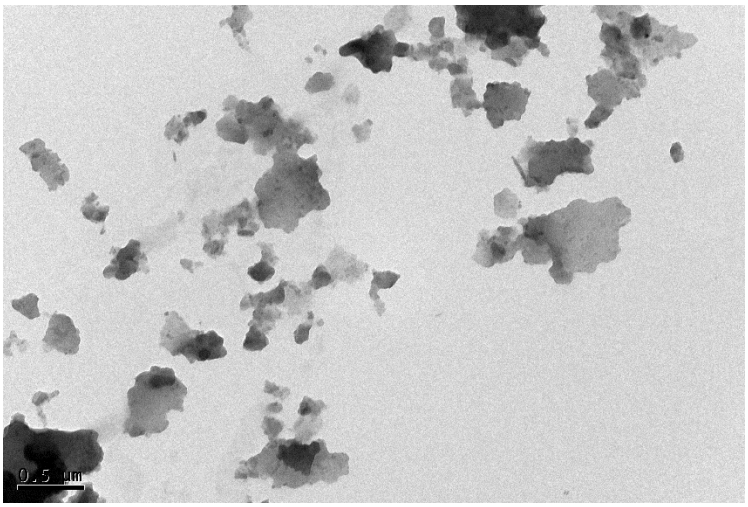


**Fig. S1** TEM image of CC nanoparticles.

**Table S1 Particle size, PDI, and zeta potential of different batches of CC nanoparticles.**

| Batches of CC nanoparticles | Particle size (nm) | PDI | Zeta potential (mV) |
|---|---|---|---|
| Batch 1 | 458.60±7.49 | 0.18±0.02 | 24.10±0.87 |
| Batch 2 | 430.13±8.08 | 0.19±0.02 | 25.03±0.31 |
| Batch 3 | 448.23±5.52 | 0.24±0.03 | 23.07±0.45 |
| Average value | 445.66±13.92 | 0.21±0.03 | 24.07±0.99 |

**Table S2 The gelation time of HPCS-C/ODEX hydrogels with different catechol group grafting rates at 25°C and 37°C.**

| **Sample** | Gelation time at 25°C (s) | Gelation time at 37°C (s) |
|---|---|---|
| HPCS-C-L/ODEX | 23.33±1.53 | 13.00±1.73 |
| HPCS-C-M/ODEX | 24.67±1.53 | 13.33±0.58 |
| HPCS-C-H/ODEX | 49.67±2.52 | 42.00±2.00 |

**Table S3 Effect of the added amount of CC nanoparticles on the crosslinking degree of hydrogels.**

| Sample | CC nanoparticles (mg/mL) | Crosslinking degree (%) |
|---|---|---|
| HPCS-C/ODEX | 0 | 88.59±2.01 |
| HPCS-C/ODEX/CC-0.5 | 0.5 | 88.14±0.45 |
| HPCS-C/ODEX/CC-1 | 1.0 | 87.87±1.52 |
| HPCS-C/ODEX/CC-2 | 2.0 | 86.73±0.59 |

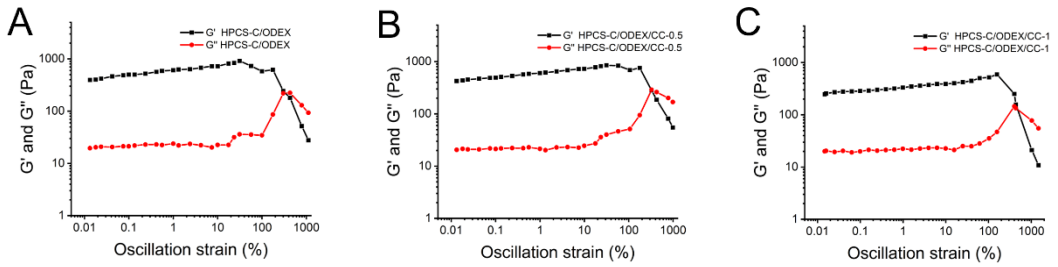


**Fig. S2** Storage modulus (G') and loss modulus (G") of (A) HPCS-C/ODEX, (B) HPCS-C/ODEX/CC-0.5, and (C) HPCS-C/ODEX/CC-1 hydrogel at oscillatory strain sweeps.

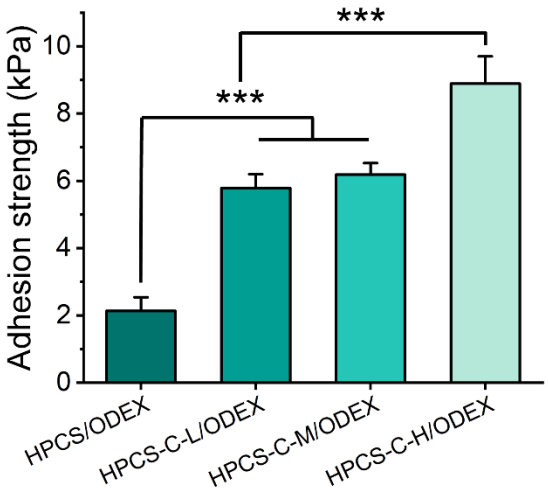


**Fig. S3** Adhesion strength of HPCS/ODEX hydrogel and HPCS-C/ODEX hydrogels with different catechol group grafting rates (n = 3, ***p < 0.001).

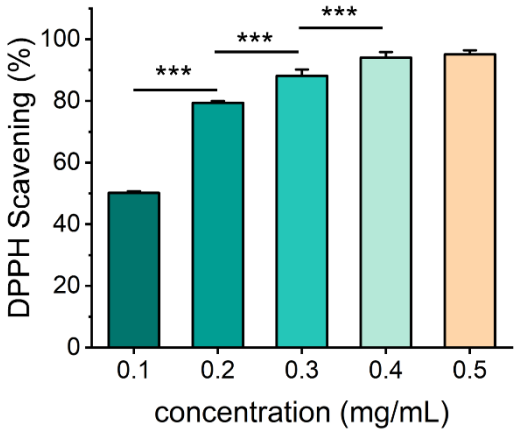


**Fig. S4** DPPH scavenging rate of different concentrations of CC nanoparticles (n = 3, ***$p < 0.001$).

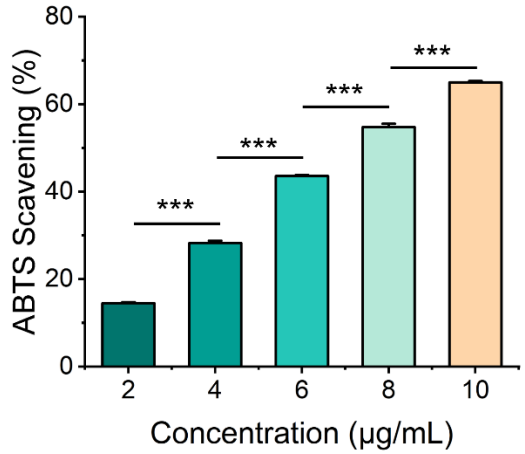


**Fig. S5** ABTS scavenging rate of different concentrations of CC nanoparticles (n = 3, ***$p < 0.001$).

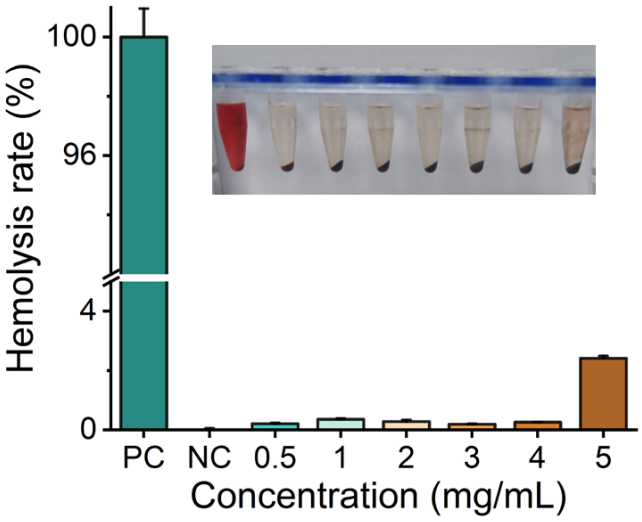


**Fig. S6** Hemolysis rates of positive control (PC, deionized water), negative control (NC, normal saline), and different concentrations of CC nanoparticles (n = 3). The insets are photographs of the hemolytic effect of PC, NC, and different concentrations of CC nanoparticles.

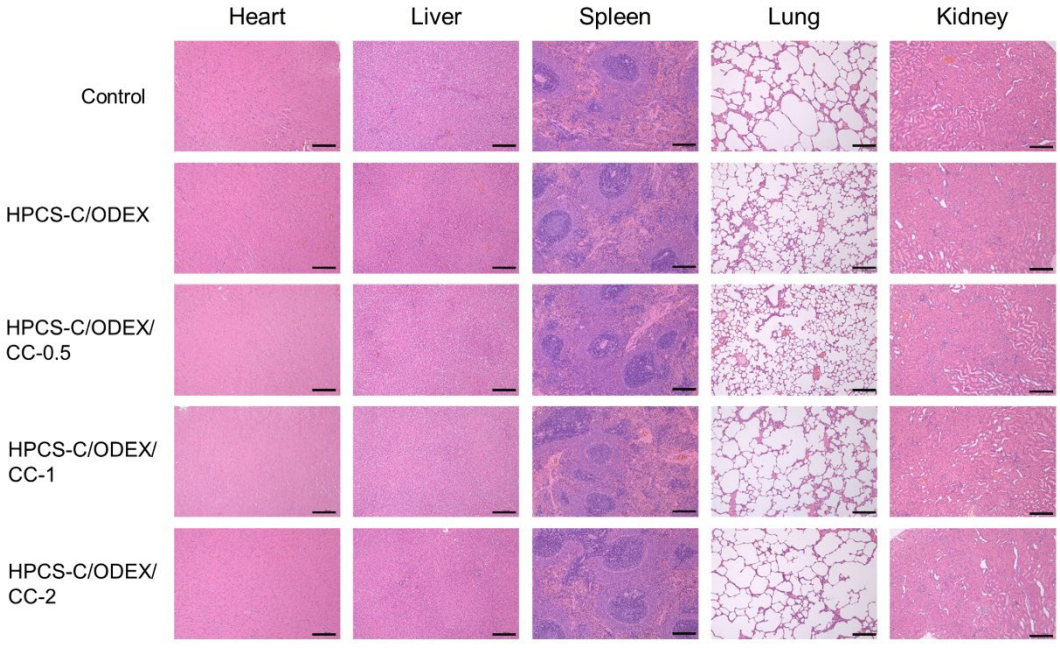


**Fig. S7** H&E staining of vital organs (heart, liver, spleen, lung, and kidney) in rats after 6 weeks of subcutaneous implantation with different hydrogels (scale bar: 200 μm).

**Table S4 Comparison of hemostasis effects of hydrogels in this work with previous reports in the literature (rat liver hemorrhage model).**

| Material name | Blood clotting time (s) | Blood loss mass in the control group (mg) | Blood loss mass (mg) | Reduction rate of blood loss mass vs. control (%) | Reference |
|---|---|---|---|---|---|
| OSA/Gel/HNTs hydrogels | 241.2 ± 15.6 | 580 ± 130 | 310 ± 60 | 46.55 | [2] |
| HGO-15-C hydrogels | 56 ± 5 | 522 ± 19 | 121 ± 8 | 76.82 | [3] |
| AOT hydrogel | 60 | 326.4 ± 58.0 | 50.2 ± 10.2 | 84.62 | [4] |
| CMC-DA/TA-1.6 hydrogel | 81 ± 4 | 830 ± 95 | 273 ± 78 | 67.11 | [5] |
| PBCO hydrogel | 31.2 | 650 | 220 | 66.15 | [6] |
| L-COC hydrogel | 69.0 ±2.9 | 1990 ± 180 | 620 ± 110 | 68.84 | [7] |
| CSGO3 hydrogel | 90 ± 26.5 | 1100 ± 282.8 | 233.3 ± 47.1 | 78.82 | [8] |
| CS-PEG-HA hydrogel | - | 382.02 ± 29.14 | 138.31 ± 33.16 | 63.79 | [9] |
| QCSMA/DAMA3/Zn-nWH2 hydrogel | 129 ± 22 | 147 ± 31 | 27 ± 5 | 81.63 | [10] |
| CS-DA/PF/TA/3D-Exo hydrogel | 47 ± 3.46 | 345 ± 32.09 | 93.33 ± 10.80 | 72.95 | [11] |
| GGB-CT hydrogel | - | 649 ± 127.9 | 177.7 ± 19.1 | 72.62 | [12] |
| CSO hydrogel | 83 ± 6 | 1300 ± 140 | 470 ± 20 | 63.85 | [13] |
| **HPCS-C/ODEX/CC-2 hydrogel** | **24.33 ± 4.16** | **243.07 ± 4.36** | **13.77 ±3.52** | **94.33** | **This work** |

## Reference


1. Y. Wang, S. Chen, Y. Yao, N. Wu, M. Xu, Z. Yin, Y. Zhao and Y. Tu, *Int. J. Biol. Macromol.*, 2023, **229**, 268-281.
2. X. Lin, D. Zhang, X. Chen and M. Liu, *ACS Sustain. Chem. Eng.*, 2024, **12**, 11739-11753.
3. L. Sun, J. Zhou, J. Lai, X. Zheng, H. Wang, B. Lu, R. Huang and L. M. Zhang, *Adv. Funct. Mater.*, 2024, **34**, 2303997.
4. H. Wang, M. Wang, J. Wu, S. Zhu, Y. Ye, Y. Liu, K. Li, R. Li, Y. Zhang, M. Wei, X. Yang and L. Meng, *Adv. Healthc. Mater.*, 2024, **13**, 2304444.
5. H. Xie, G. Shi, R. Wang, X. Jiang, Q. Chen, A. Yu and A. Lu, *Carbohydr. Polym.*, 2024, **334**, 122014.
6. J. Li, Y. Zhai, J. Xu, X. Zhu, H. Yang, H. Che, C. Liu and J. Qu, *Int. J. Biol. Macromol.*, 2024, **259**, 129006.
7. J. Yang, T. Wang, L. Zhang, P. Fan, J. Zhao, X. Zheng, Y. Lai, H. Liu and S. Wang, *J. Colloid Interface Sci.*, 2024, **673**, 395-410.
8. W. Feng and Z. Wang, *Carbohydr. Polym.*, 2022, **294**, 119824.
9. H. Li, X. Zhou, L. Luo, Q. Ding and S. Tang, *Carbohydr. Polym.*, 2022, **281**, 119039.
10. E. Yang, W. Hou, K. Liu, H. Yang, W. Wei, H. Kang and H. Dai, *Carbohydr. Polym.*, 2022, **291**, 119631.
11. H. Peng, H. Li, X. Zhang, J. Tang, Y. Liang, L. Qiao, Y. Zhu, M. Hou, S. Wei, Z. Zhang, C. Liu, X. Li, B. Liang, B. Song, B. Guo and J. Zhang, *Chem. Eng. J.*, 2023, **475**, 146238.
12. D. Xie, C. Hu, C. Jiang, J. Xia, L. Ye, Y. Jin, S. Jiang, Y. Ji, Z. Zhang, H. Song, Y. Zhu, P. Tang, Z. Hu, Y. Xiao, J. Dai and Z. Hu, *Chem. Eng. J.*, 2023, **476**, 146788.
13. M. Xie, Y. Zeng, H. Wu, S. Wang and J. Zhao, *Int. J. Biol. Macromol.*, 2022, **219**, 1337-1350.